Rapid fabrication of on-demand high-resolution optical masks with a CD–DVD pickup unit

Lucia Cabriales, Mathieu Hautefeuille,* Gerardo Fernández, Victor Velázquez, Marcela Grether, and Enrique López-Moreno

Facultad de Ciencias, Universidad Nacional Autónoma de México, Circuito Interior, Ciudad Universitaria, 04360 México DF, Mexico

*Corresponding author: mathieu_h@ciencias.unam.mx

Received 12 November 2013; revised 5 February 2014; accepted 11 February 2014; posted 12 February 2014 (Doc. ID 201232); published 18 March 2014

A low-cost, direct fabrication technique with a micrometer range resolution has been implemented for rapid prototyping of optical masks for photolithography and structured light and diffraction optics applications. Using a setup based on the optical unit of a compact disc–digital versatile disc burner, a low-energy infrared laser beam was focused on a thin polymeric layer with embedded absorbing carbon nanopowder coated on a transparent glass substrate. This allowed for the generation of a custom-made transparent pattern in a computer numerical control fashion. In addition to its great simplicity and repeatability, the method also enables grayscale contrasts for each pixel individually, and fabricated masks proved to resist high intensities. © 2014 Optical Society of America

OCIS codes: (230.1950) Diffraction gratings; (140.3390) Laser materials processing.
http://dx.doi.org/10.1364/AO.53.001802

1. Introduction

High-resolution optical masks are increasingly required for applications like photolithography and the generation of diffraction patterns in optics. Although great resolutions have been made possible with advances in microfabrication, simple and rapid fabrication processes are thus currently necessary for complex, personalized masksets fabrication [1]. Printing the desired pattern on acetates or projecting them on a substrate with a commercial projector are rapid, low-cost solutions that are generally used to produce custom-made masks, but they only offer a limited resolution in the majority of the cases [2,3]. Moreover, printed masks may be susceptible to degradation by exposure to ultraviolet light or to the environment. Efforts have been made recently to process high-resolution diffraction masks by computer generated holograms for instance, especially for dynamics optics and to produce beams carrying orbital angular momentum (OAM) [4]. However, although spatial light modulators offer great modularity and control in the generation of the desired patterns, they present an elevated cost. Thanks to the development of laser technology in recent years, short-pulsed lasers are emerging as one of the most used tools for microfabrication and micromachining. Direct laser writing is thus a practical alternative to fabricate optical masks because it allows for a reduction in the processing cost and time while optimizing the resolution [5]. However, this technology may also present some limitations, such as the initial investment cost.

In summary, all the current techniques employed to produce custom-made masks for diffraction or structured beams applications generally require costs that are proportional to the sought resolution. This typically constrains the range of possible applications in most teaching and research laboratories. In this work, efforts were made to develop a rapid-prototyping technique that allows for the fabrication of robust, custom-made, high-resolution optical masks for diffraction, photolithography, and

1559-128X/14/091802-06$15.00/0

structured light applications at a very low cost. After coating a transparent layer with a black nanocarbon-polymer composite, a laser-induced incandescence process was used to etch transparent windows in the black coating with a recycled compact disc (CD)–digital versatile disc (DVD) optical pickup unit (OPU). We present the fabrication process of several optical mask designs developed thanks to a precise control of lasing conditions and a programmable computer numerical control. These high contrast masks were successfully produced with a micrometer size resolution to demonstrate the versatility of our process in the production of any type of mask in only a few minutes. Optical characterization of the etched features as well as their resulting performance for diffraction, structured light applications, and photolithography applications are presented.

2. Experimental Procedure

A. Laser Setup

The laser setup used in this work was based on a commercial CD–DVD OPU mounted on a tridimensional displacement stage motorized with two stepper motors of micrometric resolution [6]. This homemade platform allowed us to precisely focus the beam of one of the two available wavelengths (650 and 785 nm) on a desired sample that was etched in a computer numerical control (CNC) fashion. The platform also offers control of the output power and pulse time of the laser diode to correctly adjust laser ablation conditions to specific sample and material properties. Finally, a visualization stage consisting of a 20× microscope objective attached to a charge coupled device (CCD) sensor recycled from a commercial webcam was implemented for real-time observation of the ablation process in the sample on a computer screen.

B. Sample Preparation

The dark layer of the optical masks fabricated here consisted of a clean, transparent glass slide coated with a thin black layer of carbon nanoparticles (CNPs) that blocked visible light efficiently. CNPs (carbon nanopowders, Sigma Aldrich, part number: 633-100) were incorporated and mixed with a low-cost polyester-based matrix (MPS-95, Polyformas Plasticas S.A. de C.V.) until a black paste was obtained. The mixture was cast on a clean glass substrate using the doctor blade technique with a thin razor blade [7]. After drying for 10 min at ambient conditions, the process resulted in the formation of a thin layer of a few micrometers, which was measured by profilometry (Dektak II). The choice of such a particular polymeric matrix was justified by the low cost, ease of use, and relatively low thermal conductivity ($\kappa \sim 0.2\ \mathrm{W/m \cdot K}$ for polyester) of this material. This indeed allows for the avoidance of thermal transport from the focal spot and promotes laser-induced incandescence in superficial carbon microclusters as described in [8]. Thanks to this particular polymeric matrix, the dark layer with embedded CNP was also very resistant to manipulation by hand and tweezers. Moreover, it withstood laser intensities much greater than all of the conventional commercial diffraction masks available in our laboratory. For instance, a 5 W CO_2 laser beam with a 3 cm diameter was shone onto the layers without causing any visible damage to the mask.

C. Mask Fabrication Principle

In order to etch high-resolution transparent patterns in the composite sample for the construction of optical masks, the red and near-infrared (NIR) laser diodes of the OPU were employed to generate laser-induced incandescence in superficial, absorbing carbon microclusters [6,8]. The laser spot was then focused on the desired absorbing region and ablation successfully occurred, which left a localized opening window in the otherwise opaque nanocarbon composite layer [Fig. 1(b)]. This selective etching was then used to transfer monochrome bitmaps pixel by pixel and produce more complex transparent patterns thanks to the CNC capability of the platform [Fig. 1(c)]. The pixel size was controlled after characterization of the influence of lasing conditions on the resulting resolution. This rapid prototyping fabrication process thus allowed for the production of several optical masks of a 1 mm × 1 mm area in approximately 30 min per design. More than 50 designs were then created on a single glass slide, which demonstrates that this technique permits the use of small amounts of substrate material.

3. Results

A. Characterization of the Fabricated Masks

The high-resolution masks fabricated in this work were produced using a laser-induced incandescence process adapted from [8]. The ablated pixel size was found to be dependent on the laser wavelength, correct focusing, power density, and dwell time. All of

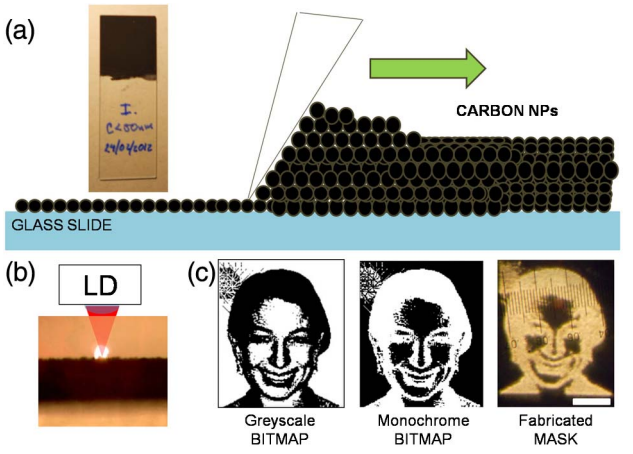

Fig. 1. (a) Diagram of the fabrication of the dark CNP composite layer on glass, (b) laser-induced incandescence process on the composite layer, and (c) CNC laser transfer of a bitmap pattern. Scale bar is 100 μm long.

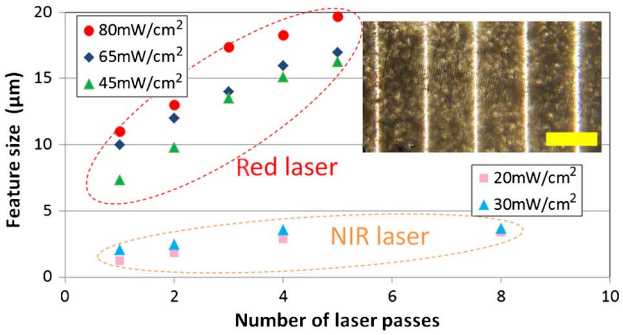

Fig. 2. In-plane feature resolution as a function of laser wavelength, power density, and number of passes. Pulse time was 5 ms. Inset shows an example of parallel lines etched with different laser passes (scale = 100 μm).

these parameters were controllable with the constructed platform. Continuous wave laser excitation can also be used to etch patterns, but this process is not repeatable and results in feature sizes that are too large for mask fabrication. Several laser pulse times were tested for the purpose of mask fabrication. Although the pixel resolution is also dependent on this parameter, the optimal adjustment of pixel size was possible by shining the laser several times at a fixed position and at a fixed dwell time of 5 ms. Figure 2 shows the relationship between etched pixel size and laser power density for the two different lasers of the OPU and for different numbers of passes. As previously observed in [8], laser-induced incandescence and subsequent etching of the film was possible at low laser power densities for the NIR wavelength while greater intensities were required when the red laser was used. Subsequently, the in-plane resolution of the ablated features was greater for the NIR laser and the number of passes greatly influenced the patterns of feature size.

Control of the laser power density and number of passes at a fixed dwell time also permitted the development of grayscale patterns as shown in the micrographs of Fig. 3, which were obtained from an optical and scanning electron microscope (SEM, Jeol JSM5600 LV) coupled to an energy dispersive spectrophotometer (EDS) working at 20 keV (NORAN Instruments). The level of transparency, contrast, and resolution of the features was clearly enhanced by increasing the number of laser passes. The overall quality of etched patterns was also increased by the number of passes as the dimension of microscopic spheres, which were visible as white spots in the SEM micrographs and probably caused by polymer heating, was drastically lowered after four passes.

It was found that this contrast was caused by the amount of composite layer remaining on the transparent substrate and that its thickness was directly dependent on the laser conditions. Unfortunately, it was difficult to measure the depth of the etched patterns with atomic force microscopy because of the high surface roughness found on the nonetched coating layer that damaged the tips. The initial layer indeed presented clustered aggregates that were visible in optical and scanning electron micrographs (see inset of Fig. 2 for an example). However, this nonhomogeneity did not impede the fabrication of the optical masks, as the conditions of the laser etching process may be controlled to limit the formation of aggregates after ablation (see Fig. 3). Small unwanted defects still remained in the openings in the best cases after laser etching, and this may affect diffraction results and micrometer-scale patterns transferred with projection or contact photolithography. These defects were identified in the SEM micrographs using detection of backscattered electrons (Fig. 4). The quality of the resulting etched features has been addressed using image processing software (ImageJ). The optimal lasing conditions guaranteed a defect density of approximately 1–10 defects/mm^2 with an average defect size of 1.78 μm and a maximal defect size of 5.2 μm. In this optimal case, the nanoparticle–polymer composite coating the transparent glass substrate permitted the transfer of single pixels with a resolution of up to 1.2 μm in the ideal case as can be seen at the bottom of the one-pixel line shown in Fig. 4(a).

B. Diffraction Masks

A series of conventional diffractive optical masks was fabricated using the laser-induced incandescence technique. A 633 nm He–Ne laser (05LHP991, Melles Griot) beam was passed through a 25 μm

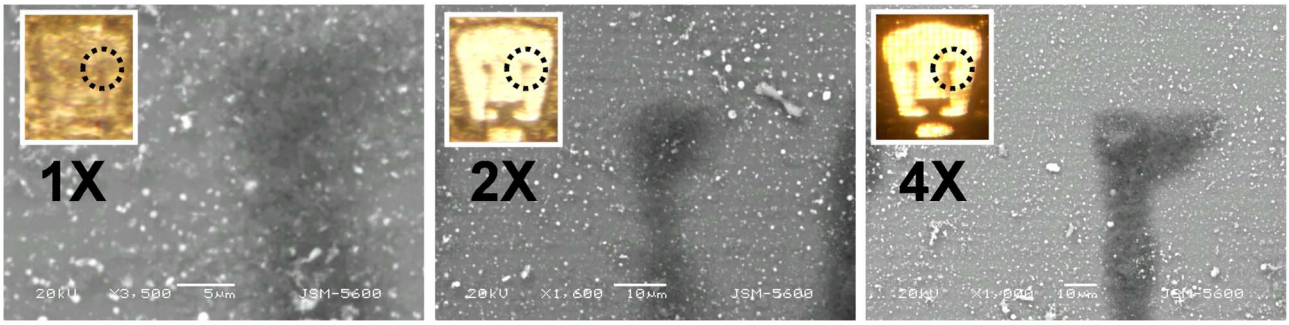

Fig. 3. Optical micrographs and SEM details of grayscale patterns after one (1×), two (2×), and four (4×) NIR laser passes of the NIR laser at 30 mW/cm^2 with a 5 ms pulse. Insets are micrographs taken with an inverted optical microscope and illumination with a 40 W white light bulb.

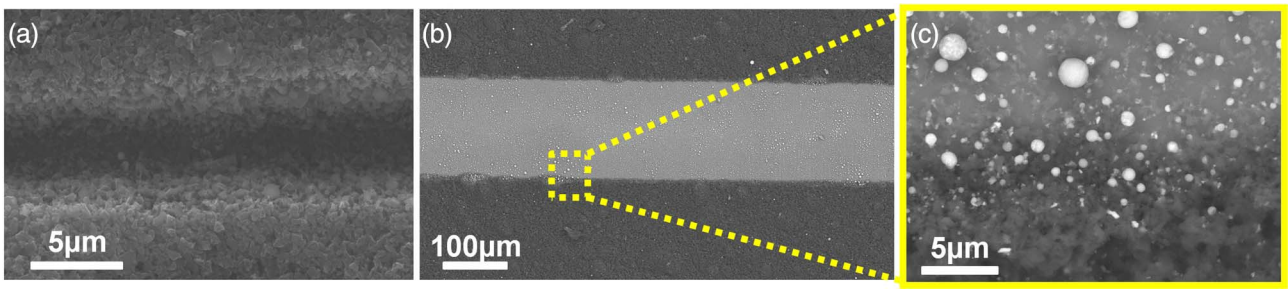

Fig. 4. (a) SEM micrograph of the detail of a "one-pixel" line etched with the CNC platform. (b) Larger laser-etched opening with (c) visible microsphere defects.

pinhole for spatial filtering and purifying of the profile before passing it through the optical diffractive mask. The resulting diffraction patterns were then projected on a CCD sensor of a commercial digital camera located at a 30 cm distance from the mask. This setup permitted us to record the largest pattern possible on a digital photograph. The lens of the camera was previously removed and the exposure time adjusted to avoid saturation and ensure correct recording. Figure 5 shows a triple slit optical mask (slits are 1 mm long, 80 μm wide, and are separated by 120 μm) with its respective diffraction pattern. This figure also compares the theoretical results with experimental ones, which showed good matching and a low loss of visibility.

OAM optical masks have also been successfully generated using fork dislocations at the center of the pattern, as mentioned in [9]. The technique proved to be very useful for this kind of experiment as it usually requires custom-made, expensive masks or spatial light modulators. It was indeed possible to design several fork-like patterns and observe the influence of different designs, as can be seen in Fig. 6. It can clearly be seen that the resolution of the masks greatly influenced the quality of the corresponding diffraction patterns and that information was lost

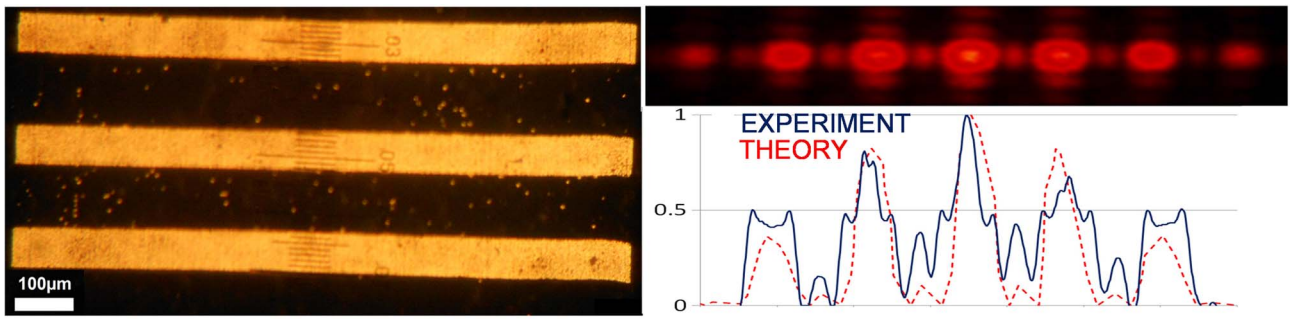

Fig. 5. Example of a three-slit optical mask and its respective diffraction pattern. Normalized intensity profile of experimental results (solid line) is compared with theory (dashed line).

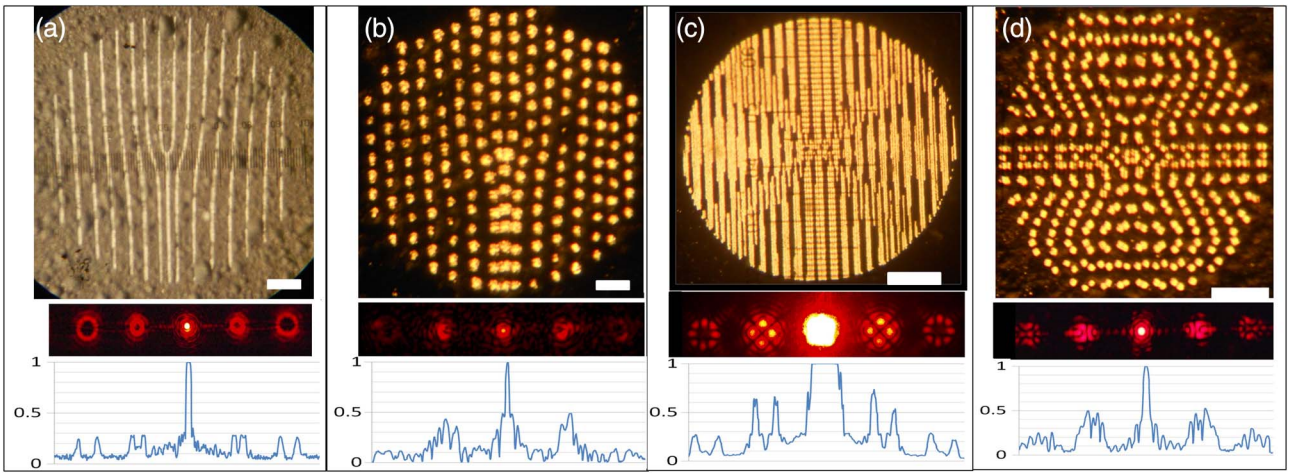

Fig. 6. Examples of fork-like diffraction masks and their corresponding patterns. Micrographs were recorded using an optical microscope and a digital camera by (a) light reflection and (b)–(d) transmission. Scale bars of micrographs are 100 μm long.

when the fork-dislocation masks were discretized into small dots. However, the complete characterization of these OAM patterns was outside the scope of this paper and will be discussed elsewhere.

C. Photolithography Masks

Finally, the possible application of the laser-etched masks in photolithography was characterized using a 365 nm sensitive resin (Loctite 3525, Henkel) soluble in acetone and a compact ultraviolet-lamp (UVG-11, UVP). The performance of the nonetched composite layers as ultraviolet (UV) filters and the etched areas as proper opened windows was first studied. Large patterns with a characteristic dimension of 1 mm were etched with up to four laser passes at maximum laser output power in order to test the features height caused by the grayscale levels. The transmission of the UV light through the glass substrate, coating composite layer, and laser-etched layers was characterized prior to the experiment with a spectrophotometer coupled to an optical fiber (HR4000, Ocean Optics). The presence of residual materials on the laser-etched mask was clearly evidenced by the absorption of deeper UV light at 254 nm, which is characteristic of carbon nanotube absorption [10]. However, the etched features proved to be useful to achieve photo-polymerization of the resin at the wavelength of interest (365 nm); more than 90% of that light was completely blocked by the black regions while 73.3% was transmitted through the etched ones. It was then been possible to generate height profiles with a unique 90 s exposure of the resin to the UV source by etching the same patterns with different numbers of laser passes. This modified the transparency of the mask's window pattern, similar to a grayscale mask [11]. The fabricated samples were thus used as contact photolithographic masks as depicted in Fig. 7, where the resulting profile heights of the corresponding transferred features are also presented. These results were compared with profiles obtained with the same procedure but using a printed grayscale optical mask. In the latter case, the patterns were printed on a commercial 500-μm-thick acetate sheet using a commercial laser printer (DocuColor 252, XEROX) and subsequently attached to a similar glass slide. Unfortunately, it was impossible to test the performance of our laser-etched masks in transferring high-resolution planar features or high aspect ratios into the resin because of the unavailability of a high-resolution stepper or precise mask aligner in our laboratory. Patterns from 1 mm to 100 μm were indeed successfully transferred with limited exposure imperfections, whereas the results with smaller features were not satisfactory. The observed deformities were probably caused by the poor quality of light source collimation in our experimental optical setup, i.e., refraction inside the glass substrate. The role played by the residual materials after laser etching should also be characterized with proper photolithographic equipment in the future.

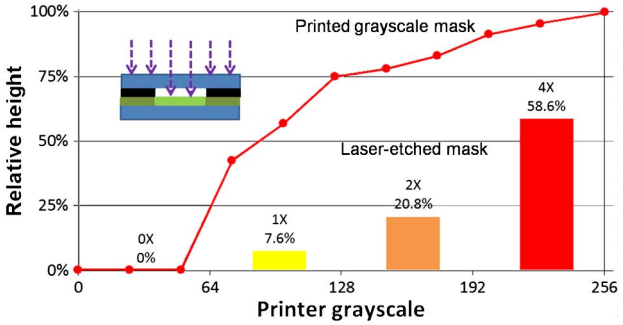

Fig. 7. Relative height of photolithographic patterns transferred in a Loctite 3525 resin obtained with a laser-etched mask and a printed grayscale mask.

4. Conclusion

Low-cost, rapid fabrication of personalized optical masks has been made possible in less than 30 min thanks to a custom-made laser platform based on a CD–DVD pickup unit. Using a simple method, transparent opening windows were etched in a nanocarbon-based dark composite that completely blocks visible and UV light. Many different on-demand designs were then successfully fabricated on a single glass slide substrate coated with this layer, thus offering a simple solution for the realization of simple optical diffraction experiments at a low cost and usable by almost anyone. More complex features were also tested for the generation of optical masks for orbital angular momentum diffraction experiments and photolithography, and these showed promising results.

The authors are grateful to DGAPA-UNAM for partial funding of the project (PAPIIT grant IN116914). We also thank Margarita Rivera, Carlos Magaña, and Mario Monroy Escamilla for their technical help during SEM sessions and Reinher Pimentel-Domínguez for all the constructive discussions.

References

1. D. Qin, Y. Xia, A. J. Black, and G. M. Whitesides, "Photolithography with transparent reflective photomasks," J. Vac. Sci. Technol. B **16**, 98–103 (1998).
2. E. Orabona, A. Caliò, I. Rendina, L. De Stefano, and M. Medugno, "Photomasks fabrication based on optical reduction for microfluidic applications," Micromachines **4**, 206–214 (2013).
3. J. D. Musgraves, B. T. Close, and D. M. Tanenbaum, "A maskless photolithographic prototyping system using a low-cost consumer projector and a microscope," Am. J. Phys. **73**, 980–983 (2005).
4. D. G. Grier, "A revolution in optical manipulation," Nature **424**, 810–816 (2003).
5. Y. Li, Y. Dou, R. An, H. Yang, and Q. Gong, "Permanent computer-generated holograms embedded in glass by femtosecond laser pulses," Opt. Express **13**, 2433–2438 (2005).
6. M. Hautefeuille, A. K. Jimenez-Zenteno, P. Perez-Alcazar, K. Hess-Frieling, G. Fernandez-Sanchez, V. Velazquez, M. Grether, and E. Lopez-Moreno, "Utilization of a digital-versatile-disc pickup head for benchtop laser microfabrication," Appl. Opt. **51**, 1171–1177 (2012).

7. M. A. Aegerter and M. Mennig, eds., *Sol-Gel Technologies for Glass Producers and Users* (Springer, 2004).
8. M. Hautefeuille, L. Cabriales, R. Pimentel-Domínguez, V. Velázquez, J. Hernández-Cordero, L. Oropeza-Ramos, M. Rivera, M. P. Carreon-Castro, M. Grether, and E. López-Moreno, "New perspectives in direct PDMS microfabrication using a CD–DVD laser," Lab Chip **13**, 4848–4854 (2013).
9. A. M. Yao and M. J. Padgett, "Orbital angular momentum: origins, behavior and applications," Adv. Opt. Photon. **3**, 161–204 (2011).
10. S. C. Singh, H. B. Zeng, C. Guo, and W. Cai, eds., *Nanomaterials: Processing and Characterization with Lasers* (Wiley, 2012).
11. T. J. Suleski and D. C. O'Shea, "Gray-scale masks for diffractive-optics fabrication: I. Commercial slide imagers," Appl. Opt. **34**, 7507–7517 (1995).